Bioorganic & Medicinal Chemistry Letters 22 (2012) 2063–2069

Contents lists available at SciVerse ScienceDirect

Bioorganic & Medicinal Chemistry Letters

journal homepage: www.elsevier.com/locate/bmcl

Discovery of azabenzimidazole derivatives as potent, selective inhibitors of TBK1/IKKε kinases

Tao Wang [a,*], Michael A. Block [a], Scott Cowen [a], Audrey M. Davies [a], Erik Devereaux [b], Lakshmaiah Gingipalli [a], Jeffrey Johannes [a], Nicholas A. Larsen [b], Qibin Su [a], Julie A. Tucker [c], David Whitston [b], Jiaquan Wu [b], Hai-Jun Zhang [a], Michael Zinda [b], Claudio Chuaqui [a,*]

[a] Department of Cancer Chemistry, Oncology Innovative Medicines Unit, AstraZeneca R&D Boston, 35 Gatehouse Drive, Waltham, MA 02451, USA
[b] Department of Cancer Bioscience, Oncology Innovative Medicines Unit, AstraZeneca R&D Boston, 35 Gatehouse Drive, Waltham, MA 02451, USA
[c] Discovery Sciences, AstraZeneca R&D, Alderley Park, Cheshire, United Kingdom

ARTICLE INFO

Article history:
Received 11 November 2011
Revised 3 January 2012
Accepted 9 January 2012
Available online 14 January 2012

Keywords:
TBK1
IKKε
Azabenzimidazole
Kinase inhibitor

ABSTRACT

The design, synthesis and biological evaluation of a series of azabenzimidazole derivatives as TBK1/IKKε kinase inhibitors are described. Starting from a lead compound **1a**, iterative design and SAR exploitation of the scaffold led to analogues with nM enzyme potencies against TBK1/IKKε. These compounds also exhibited excellent cellular activity against TBK1. Further structure-based design to improve selectivity over CDK2 and Aurora B resulted in compounds such as **5b–e**. These probe compounds will facilitate study of the complex cancer biology of TBK1 and IKKε.

Protein kinases are important members of the encoded human genome that are involved in the regulation of normal and pathophysiological processes.[1,2] One sub-family of the ca. 500 membered protein kinases is the IκB kinases which consists of five isoforms: IKKα, IKKβ, IKKγ, IKKε and TBK1. These IκB kinases serve as the critical components in the NF-κB activation pathway that leads to RELA/B activation and the regulation of cell proliferation, survival, innate and adaptive immune responses.[3] Among these five members, IKKγ lacks kinase domain while IKKα and IKKβ have been extensively studied and targeted using small molecule inhibitors for the treatment of cancer and other diseases.[4] Besides the NF-κB pathway, TBK1 and IKKε were shown to be essential components of the interferon regulatory factor 3 (IRF3) signaling pathway.[5]

TBK1 and IKKε have attracted great interest in the cancer area in recent years. It was reported that TBK1 kinase activity was up-regulated in certain transformed cells and that TBK1 was required for the survival of these cells in culture.[6,7] An integrative genomic approach that incorporated an overexpression screen, RNAi screen and comparative genomic analysis identified IKKε as an oncogene in human breast cancer, and showed that suppression of IKKε expression in breast cancer cell lines with IKKε amplifications induced cell death.[8] A recent report showed that IKKε and TBK1 act together by phosphorylating AKT in a PI3K signaling dependent manner and that the dual phosphorylation resulted in a robust AKT activation in vitro.[9] So far there have been few reports on small molecule inhibitors of TBK1 and/or IKKε.[10–12] We herein report the discovery of a novel series of azabenzimidazole derivatives as potent and selective TBK1/IKKε kinase inhibitors.

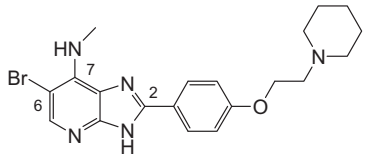

1a

Figure 1. Azabenzimidazole hit from screening.

Screening of a kinase focused subset of the AstraZeneca compound collection against the TBK1 enzyme identified compound **1a** as an initial hit (Fig. 1). Compound **1a** had an IC_{50} of 0.151 μM against the TBK1 enzyme. Compound **1a** was also active against IKKε (IC_{50}: 0.707 μM). A homology model of TBK1 was built using Prime v.1.5[13] based on the structure of PAK4 (AstraZeneca proprietary structure, unpublished data). A proposed binding mode for the azabenzimidazole scaffold was generated using Glide v.4.5[14] where the inhibitor binds to the hinge of the kinase via the pyridine

* Corresponding authors. Tel.: +1 781 839 4734; fax: +1 781 839 4230 (T.W.); tel.: +1 781 839 4106; fax: +1 781 839 4230 (C.C.).
E-mail addresses: tao.wang@astrazeneca.com (T. Wang), claudio.chuaqui@astrazeneca.com (C. Chuaqui).

0960-894X/$ - see front matter © 2012 Elsevier Ltd. All rights reserved.
doi:10.1016/j.bmcl.2012.01.018

Table 1
Initial 6- and 7-position SAR

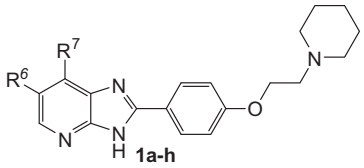

1a-h

Compd	R^6	R^7	TBK1 IC_{50} (μM)	IKKε IC_{50} (μM)
1a	Br		0.151	0.707
1b	Br	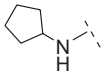	1.22	NT
1c	Br	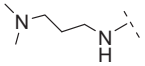	2.29	NT
1d	Br	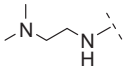	10.3	NT
1e	Br	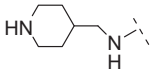	0.105	0.523
1f	Br	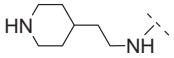	0.468	4.32
1g	CN		0.426	NT
1h	Br		2.74	NT

nitrogen and the imidazole N–H groups while the piperidine side chain is directed to the solvent. The 6-substituent (Br on **1a**) points to the gatekeeper methionine (conserved in TBK1 and IKKε) (Fig. 2).

This chemical series was attractive as three positions (2, 6 and 7-positions) on compound **1a** offered clear opportunities to develop structure–activity relationships. First, the substitution at the 2-position was fixed with a *para*-substituted phenyl moiety and the R^6 group was kept constant as Br (or CN as one matched pair) to allow the probing of SAR off the amino group at the 7-position. As the data in Table 1 show, replacement of the methyl group on **1a** with a more bulky lipophilic group (cyclopentyl on **1b**) resulted in an eightfold decrease in TBK1 enzyme activity.[15] Linear chains of variable chain length and with a polar terminal di-methylamino group also led to a significant drop in TBK1 enzyme potency (**1c** and **1d**). Interestingly, piperidine chains of variable length were tolerated in TBK1 (**1e** and **1f**). Compound **1e** also has comparable potency against IKKε as compared to that of **1a**.[15] Compound **1g** is a matched pair of **1a** and showed an IC_{50} of 0.426 μM against TBK1, suggesting that 6-cyano was at least as good as a 6-Br group. When the amino group was replaced with a simple Cl, the resulting analogue **1h** was much less potent, demonstrating the importance of the amino group at the 7-position. We conclude from this 7-position exploration that a methylamino group was one of the best groups in terms of TBK1 enzyme potency and it was kept constant to allow further SAR work at other positions.

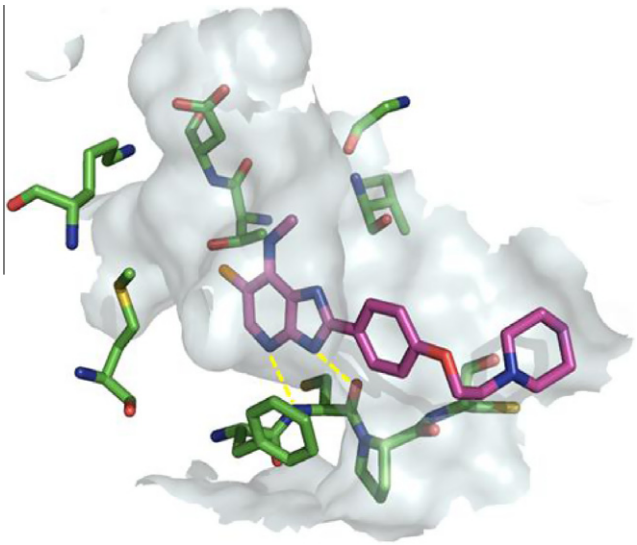

Figure 2. Azabenzimidazole hit **1a** in a TBK1 homology model.

An SAR study of the 2-position of the azabenzimidazole was carried out next. As illustrated in Table 2, removal of the methylenepiperidine moiety from **1a** gave **2a** with a comparable IC_{50} of 0.335 μM against the TBK1 enzyme. Both electron-donating and electron-withdrawing functional groups were tolerated at the 4′-position such as –OEt (**2b**), –OH (**2d**), $-CO_2H$ (**2e**) and $-SO_2Me$ (**2f**), with the exception of $-O^iPr$ (**2c**). Moving the methyl sulfone to the *meta*-position on the phenyl ring resulted in a drop of enzyme potency to 9.55 μM. However, both *meta*- and *para*-NH_2 analogues had reasonable potencies of 0.065 (**2h**) and 0.111 μM (**2i**), respectively. The phenyl ring itself could be replaced with an aminopyridine without losing activity (**2j**). Bis-substitution (such as **2k**) retained the TBK1 potency. A variety of basic side chains besides the original piperidine on **1a** were also tolerated (**2l–r**), suggesting that this area offers potential for modulating the physical properties of the inhibitor without affecting the target activities. Replacement of the phenyl ring with another aromatic system yielded both active (**2s**, indazole) and less active (**2t**, N-Me imidazole) analogues. As expected from the high sequence/binding site similarities between TBK1 and IKKε, for those analogues whose IKKε IC_{50}'s were also measured, both enzyme potencies (TBK1 and IKKε) tracked well with one another.

To determine whether the bromo was optimal at the 6-position of the azabenzimidazole, additional substitutions were explored beyond Br and cyano groups (Table 3). It was found that the 6-$CONH_2$ moiety gave an analogue with an equal TBK1 enzyme po-

Table 2
SAR of the 2-position of benzimidazoles

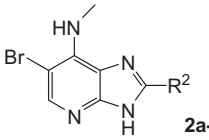

2a-t

Compd	R^2	TBK1 IC_{50} (μM)	IKKε IC_{50} (μM)	Compd	R^2	TBK1 IC_{50} (μM)	IKKε IC_{50} (μM)
2a	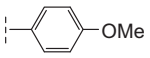	0.335	NT	**2k**	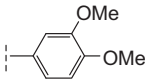	0.345	NT
2b	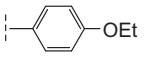	0.231	NT	**2l**	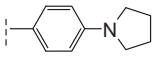	0.388	5.96
2c	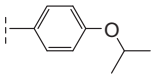	1.41	NT	**2m**	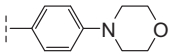	0.213	NT
2d	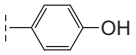	0.201	NT	**2n**	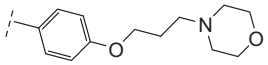	0.233	NT
2e	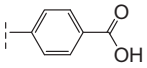	0.257	0.590	**2o**	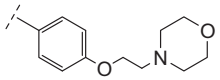	0.178	NT
2f	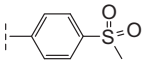	0.229	NT	**2p**	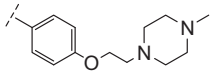	0.106	NT
2g	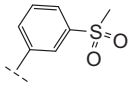	9.55	>30	**2q**	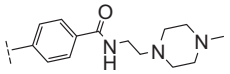	0.196	0.627
2h	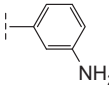	0.065	0.093	**2r**	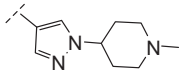	0.192	0.51
2i	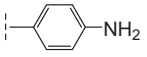	0.111	0.425	**2s**	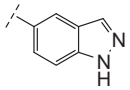	0.288	NT
2j	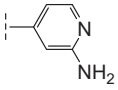	0.093	0.120	**2t**	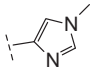	1.52	2.46

Table 3
SAR of the 6-position of benzimidazoles

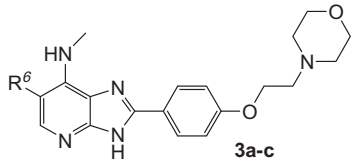

3a-c

Compd	R^6	TBK1 IC_{50} (μM)	IKKε IC_{50} (μM)
3a	$-CONH_2$	0.162	NT
2o	Br	0.178	NT
3b	Cl	0.383	16.1
3c	H	12	NT

tency (**3a**). Replacement of the Br with Cl (**3b**) resulted in a slight TBK1 enzyme potency decrease. Removal of the Br, however, rendered a loss of TBK1 activity (**3c**).

After exploration of the 2- and 6-positions of the azabenzimidazole, the SAR of the 7-position was revisited. At this point, a TBK1 reporter assay was developed to assess the cellular potency of these compounds.[16] In this cell assay, the stably transfected HEK293-TLR3 NF-κB ISRE-Luciferase cell line was stimulated with its putative ligand (in this case a synthetic dsRNA POLY I:C which recapitulates the response of viral RNA) and then treated with potential inhibitors to assess the inhibitory activity. When combined with 2-(*para*-MeO)-phenyl and 6-Br, both amino and oxygen linked piperidine side chains produced analogues with TBK1 IC_{50}s below 100 nM for the first time in this series (**4a–b** in Table 4). Their IC_{50}s against IKKε were just ~4 to 5-fold less active and the TBK1 enzyme to cell drop off was within 2 to 3-fold.

The PDK1 inhibitors BX-320 and BX-795[12] have been reported to have nM TBK1/IKKe activity.[11] From binding mode overlays in TBK1 between the azabenzimidazole scaffold (represented by **3a**) and BX-320 (Fig. 3, orange) it was reasoned that similar side chains should be evaluated at the 7-position of the azabenzimidazole scaffold. Indeed, amido side chains were reported previously on TBK1/IKKε inhibitors.[12] An analogue with 3′-acetyl-1′,3′-diamine at the 7-position (**4c**) had a TBK1 IC_{50} of 0.070 μM. Changing the terminal group of the 7-position from Me to ^{i}Pr boosted the TBK1 enzyme potency to 0.010 μM (**4d**) (Table 4). Docking studies suggest that amide substituents interact with a lipophilic region of P-loop and the alkyl side chain of the conserved Lys. The improved potency of bulkier hydrophobic groups may be rationalized by increased hydrophobic interactions between the inhibitor and the P-loop sub-pocket. Potencies against TBK1 cell and IKKε enzyme were also improved to 0.014 and 0.084 μM, respectively. A bulky alkyl terminal group (e.g., ^{t}Bu in **4e**) was also tolerated. Regarding cycloalkyl terminal groups, all 3–5-membered rings (**4f–k**) were potent and the cyclobutyl analogue **4h** had single digit nM potencies against

Table 4
SAR of the 7-position of azabenzimidazoles

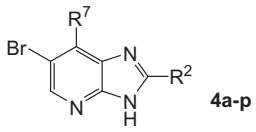

4a-p

Compd	R^7	R^2	TBK1 IC_{50} (μM)	IKKε IC_{50} (μM)	TBK1 cell EC_{50} (μM)	Aurora B IC_{50} (μM)	CDK2 IC_{50} (μM)
4a	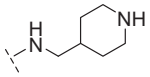	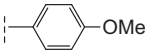	0.057	0.265	0.111	0.043	0.135
4b	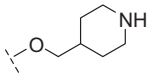		0.039	0.172	0.076	0.031	0.133
4c	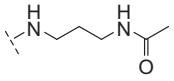		0.070	0.543	0.073	0.024	0.370
4d	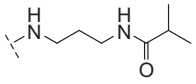		0.010	0.084	0.014	0.030	>5.28
4e	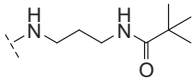		0.007	0.060	0.011	0.081	>30
4f	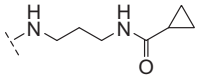		0.018	0.115	0.025	0.025	1.37
4g	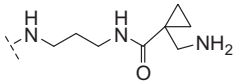		0.004	0.005	0.020	0.029	0.070
4h	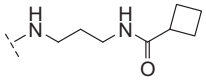		0.004	0.021	0.006	0.038	>4.91
4i	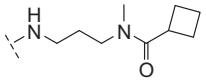		0.005	0.020	0.006	0.007	0.187
4j	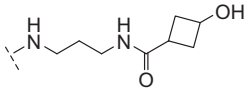		0.008	0.046	0.040	0.016	0.345
4k	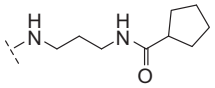		0.010	0.076	0.008	0.093	2.79
4l	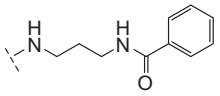		0.106	14.9	0.084	0.733	3.97
4m	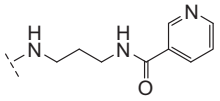		0.059	0.278	0.087	NT	NT
4n	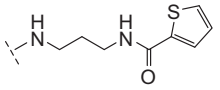		0.046	0.541	0.026	NT	NT
4o	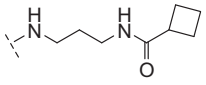	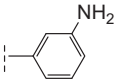	0.003	0.004	0.004	0.004	0.155
4p	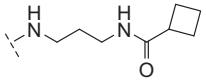	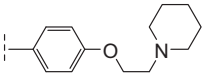	0.004	0.017	0.012	0.013	0.518

both TBK1 enzyme and cell. The hydrogen atom on the amido nitrogen was not necessary as shown with analogue **4i** (N-Me). Aryl analogues, including benzoic (**4l**) and nicotinic (**4m**) were slightly less potent as compared to the cyclobutyl analogues. When the *para*-MeO phenyl was replaced with other preferred groups based on the data shown in Table 2, highly potent analogues such as **4o** and **4p** were obtained. Compound **4d** was profiled against 79 kinases (single point at 1 μM) in order to assess the selectivity of

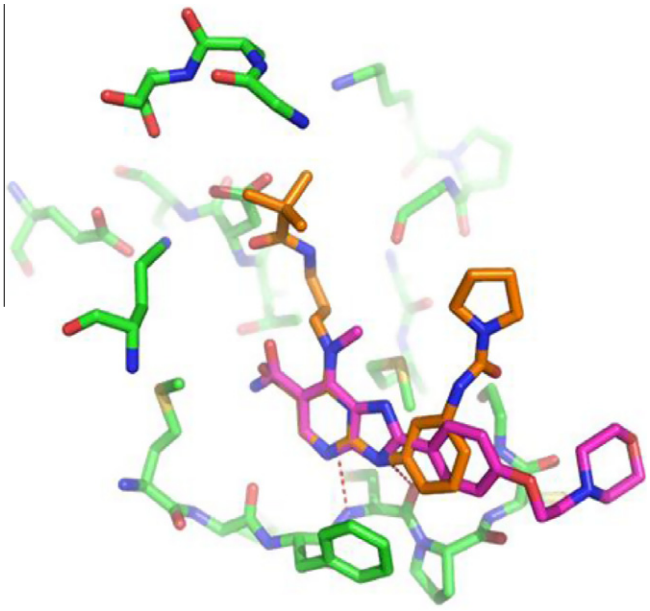

Figure 3. Overlay of azabenzimidazole **3a** with BX-320.

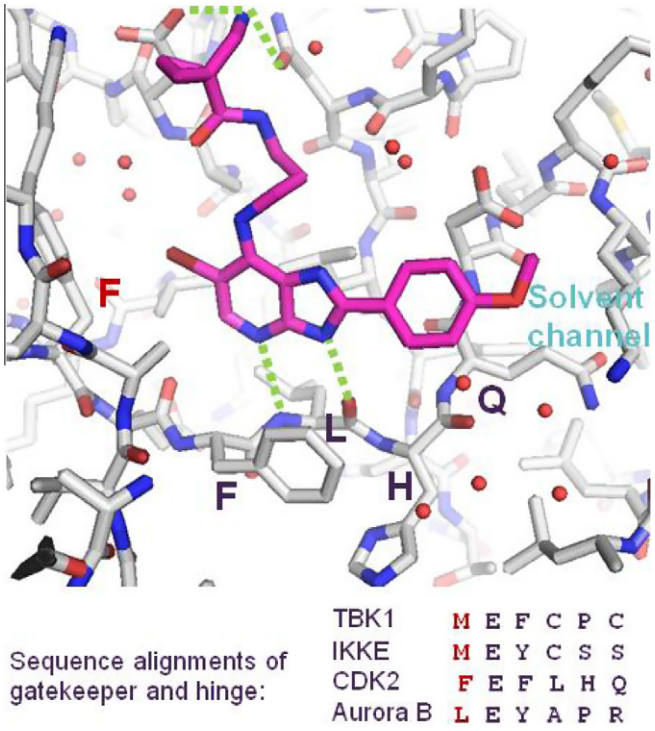

Figure 4. Compound **4g** in a CDK2 crystal structure.

the azabenzimidazole series. The Gini coefficient computed from these data is 0.556 which indicates the compound is moderately selective with six kinases being inhibited within 10-fold of TBK1.[17] As structurally related compounds were reported as weak Aurora inhibitors in the literature,[18] this series was profiled against Aurora B and CDK2 enzymes as counter screens and the data showed that most of the 7-substituted analogues in Table 4 (except for **4l** , which was also less potent against TBK1/IKKε) were potent inhibitors against Aurora B kinase at least at the enzyme evel. A majority of these analogues also had IC_{50}s of less than 1 μM against CDK2.

As both CDK2 and Aurora B kinases are important players in cell cycle progression and regulation, inhibition of those kinases would complicate our study of the effects TBK1/IKKε modulation on cancer biology. It was therefore desirable to improve the selectivity of our series over CDK2 and Aurora B kinases. A comparative binding site sequence and structural analysis between TBK1/IKKε and Aurora/CDK2 revealed several potential target sites on the protein to drive selectivity over Aurora/CDK for this series. More-

Table 5
Improvement of kinase selectivity over Aurora B and CDK2

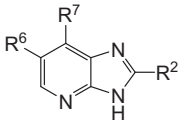

5a-e

Compd	R^6	R^7	R^2	TBK1 IC_{50} (μM)	IKKε IC_{50} (μM)	TBK1 cell EC_{50} (μM)	Aurora B IC_{50} (μM)	CDK2 IC_{50} (μM)
5a	$CONH_2$	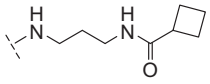	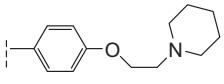	0.004	0.009	1.46	0.478	9.41
5b	$CONH_2$	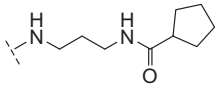	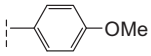	0.009	0.046	0.139	1.58	>30
5c	Br	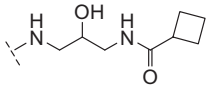		0.032	0.102	0.035	0.872	4.65
5d	Br	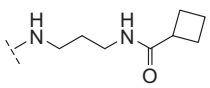	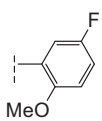	0.04	0.122	0.017	0.37	6.52
5e	Br	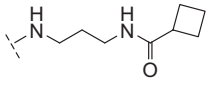	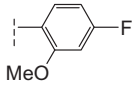	0.038	0.204	0.034	0.664	2.02

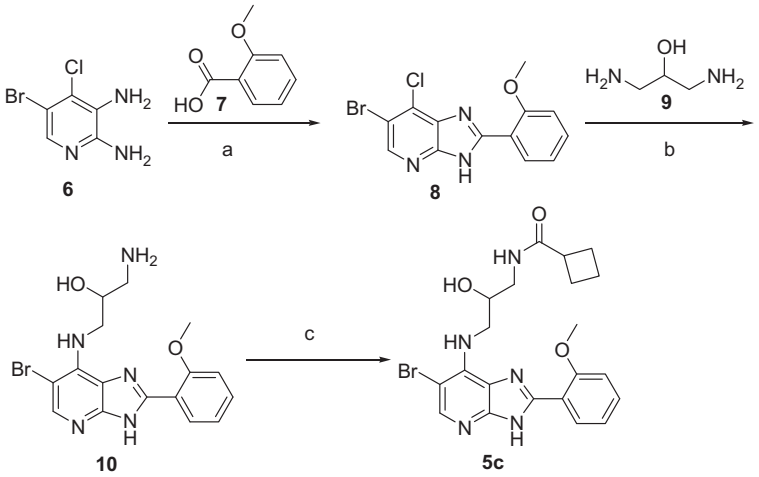

Scheme 1. Reagents and conditions: (a) 2-methoxybenzoic acid (**7**), $POCl_3$, CH_3CN, microwave, 150 °C, 1 h; (b) 2-hydroxyl-1,3-diamine (**9**, excess), *n*-BuOH, microwave, 160 °C, 4 h; (c) cyclobutanecarboxylic acid, HATU, Et_3N, DMF, room temperature, 2 h.

over, an X-ray crystal structure of **4g** in complex with CDK2 aided the design of inhibitors with reduced CDK2 potency (Fig. 4).[19] For the purpose of tuning the azabenzimidazole scaffold selectivity, the most obvious residue to exploit is the gatekeeper on the hinge which is variable for the off-target kinases: TBK1 (Met), IKKε (Met), Aurora family (Leu), and CDK2 (Phe). As shown in Figure 4, the 6-substituent of the azabenzimidazole points to the gatekeeper, therefore it was reasoned that modification off the 6-position might modulate the selectivity against the Aurora B and CDK2 kinases. As the data in Table 5 show, analogues with a 6-$CONH_2$ group (**5a–b**) exhibited significant improvements in selectivity over Aurora B and CDK2 while retaining TBK1 and IKKε enzymatic potencies. The TBK1 cellular potency for **5a** dropped to 1.46 μM presumably due to poor permeability, while analogue **5b** also gave sub-optimal potency (0.139 μM) in the TBK1 cell assay. Our second strategy to gain selectivity was through modification at the solvent channel (2-substituent of the azabenzimidazole) since there are also differences among these kinases in this region (more prominent between TBK1/IKKε and CDK2). After some library exploration work, it was discovered that the analogue with an *ortho*-MeO phenyl at the 2-position and a 7-side chain containing a hydroxyl group (**5c**) had a balanced potency profile: 0.032/0.102 μM against TBK1/IKKε; 0.035 μM in TBK1 cell assay, 0.870/4.65 μM against Aurora B/CDK2. Close analogues **5d–e** also followed the same trend. As shown above, our structure-based design approach took advantage of the differences between TBK1/IKKε and CDK2/Aurora B at both the gatekeeper position and the solvent channel and resulted in potent and selective compounds **5b–e**.

A representative synthesis of the lead compound **5c** of this series is illustrated in Scheme 1. The synthesis commenced with a tetra-substituted pyridine **6**. Treatment of **6** with **7** and $POCl_3$ in CH_3CN gave **8** with the azabenzimidazole core structure installed. Nucleophilic aromatic substitution at the 7-position of azabenzimidazole **8** with excess 2-hydroxyl-1,3-diamine **9** produced intermediate **10**, which then underwent an amide coupling reaction to yield the target compound **5c**.

In summary, a series of novel azabenzimidazole analogues was discovered and optimized against TBK1/IKKε kinases. Structure-based design targeting the gatekeeper residues and the solvent channel resulted in lead compounds (such as **5b–e**) that showed good TBK1 cellular activity and were selective for TBK1/IKKε over Aurora B/CDK2 kinases. These compounds could serve as useful probe compounds in the study of the complex cancer biology of TBK1 and IKKε kinases.

Acknowledgments

The authors would like to thank Judith Stanway for insect cell culture, Anna Valentine for protein purification, Claire Brassington for protein crystallization, Scott Williams and Melissa Vasbinder for the helpful discussions.

References and notes

1. Dancey, J.; Sausville, E. A. *Nat. Rev. Drug Disc.* **2003**, *2*, 296.
2. Zhang, J.; Yang, P. L.; Gray, N. S. *Nat. Rev. Cancer* **2009**, *9*, 28.
3. Lee, D.-F.; Hung, M.-C. *Clin. Cancer Res.* **2008**, *14*, 5656.
4. Burke, J. R. *Curr. Opin. Drug Disc. Dev.* **2003**, *6*, 720.
5. Fitzgerald, K. A.; McWhirter, S. M.; Faia, K. L.; Rowe, D. C.; Latz, E.; Golenbock, D. T.; Coyle, A. J.; Liao, S.-M.; Maniatis, T. *Nat. Immunol.* **2003**, *4*, 491.
6. Chien, Y.; Kim, S.; Bumeister, R.; Loo, Y.-M.; Kwon, S. W.; Johnson, C. L.; Balakireva, M. G.; Romeo, Y.; Kopelovich, L.; Gale, M., Jr.; Yeaman, C.; Camonis, J. H.; Zhao, Y.; White, M. A. *Cell* **2006**, *127*, 157.
7. Bodemann, B. O.; White, M. A. *Nat. Rev. Cancer* **2008**, *8*, 133.
8. Boehm, J. S.; Zhao, J. J.; Yao, J.; Kim, S. Y.; Firestein, R.; Dunn, I. F.; Sjostrom, S. K.; Garraway, L. A.; Weremowicz, S.; Richardson, A. L.; Greulich, H.; Stewart, C. J.; Mulvey, L. A.; Shen, R. R.; Ambrogio, L.; Hirozane-Kishikawa, T.; Hill, D. E.; Vidal, M.; Meyerson, M.; Grenier, J. K.; Hinkle, G.; Root, D. E.; Roberts, T. M.; Lander, E. S.; Polyak, K.; Hahn, W. C. *Cell* **2007**, *129*, 1065.
9. Xie, X.; Zhang, D.; Zhao, B.; Lu, M.-K.; You, M.; Condorelli, G.; Wang, C.-Y.; Guan, K.-L. *Proc. Natl. Acad. Sci. U.S.A.* **2011**, *108*, 6474.
10. Bamborough, P.; Christopher, J. A.; Cutler, G. J.; Dickson, M. C.; Mellor, G. W.; Morey, J. V.; Patel, C. B.; Shewchuk, L. M. *Bioorg. Med. Chem. Lett.* **2006**, *16*, 6236.
11. Bain, J.; Plater, L.; Elliott, M.; Shpiro, N.; Hastie, C. J.; Mclauchlan, H.; Klevernic, I.; Simon, C.; Arthur, J. S. C.; Alessi, D. R.; Cohen, P. *Biochem. J.* **2007**, *408*, 297.
12. Feldman, R. I.; Wu, J. M.; Polokoff, M. A.; Kochanny, M. J.; Dinter, H.; Zhu, D.; Biroc, S. L.; Alicke, B.; Bryant, J.; Yuan, S.; Buckman, B. O.; Lentz, D.; Ferrer, M.; Whitlow, M.; Adler, M.; Finster, S.; Chang, Z.; Arnaiz, D. O. *J. Biol. Chem.* **2005**, *280*, 19867.
13. *Prime, version 1.5*; Schrodinger, LLC, New York, NY, 2010.
14. Glide, version 4.5, Schrodinger, LLC, New York, NY, 2010. The homology model structure was prepared using the default protein preparation workflow. Grids were generated using the centroid of an arbitrary ligand placed in the ATP binding site incorporating hydrogen bonding constraints to the hinge. Ligands were prepared using proprietary in-house software. Docking was carried out using the XP option and constrained to make both hydrogen bonds to the hinge of the kinases. Five poses were retained for each ligand.
15. TBK1/IKKε enzyme assays: Inhibitory effect of compounds against TBK1 and IKKε was evaluated by IC_{50}s. In a typical experiment, a series of kinase catalyzed reactions with different concentrations of an inhibitor were set up in HEPES buffer with a kinase and its substrates (for TBK1, 3 nM recombinant full-length TBK1 (Life Technologies, Madison. WI), 1.8 μM CK1tide (5FAM-Ahx-KRRRAL(pS)VASLPGL, Primm Biotech, Cambridge, MA), 30 μM ATP, and 10 mM $MgCl_2$; for IKKε, 4 nM IKKε, 1.5 μM peptide substrate (5FAM-AKELDQGSLCTpSFVGTLQ-NH2, 21st Century Biochemicals, Marlborough, MA), 5 μM ATP, and 10 mM MgCl2). For 10-point IC_{50} test, inhibitor concentrations were usually started from 10 μM, followed by nine half-log dilutions. Reactions were kept at room temperature for a pre-defined duration of time, quenched using HEPES buffer containing EDTA, and then analyzed

using microfluidic mobility shift assay on a Caliper LC3000 system. The ratio of product (phosphorylated peptide) to total peptide was used to calculate percentage inhibition for each inhibitor concentration. IC_{50}s were obtained by fitting the percentage inhibition data to a four-parameter sigmoidal IC_{50} equation using Abase (IDBS).

16. TBK1 cell assay: On day 1, plate 40000 HEK293-TLR3 NF-κB-ISRE-Luciferase cells/well for a final volume 100 μL in Corning flat bottomed 96 well poly-D-lysine coated plates in DMEM containing 10% FBS. On day 2 prepare poly I:C, (1 mg/mL stock in 1 × PBS) by heating at 50 °C, mix thoroughly, use DMEM containing 0.5% FBS to dilute to a final concentration of 50 μg/mL poly I:C. The synthetic dsRNA poly I:C recapitulates the response of viral RNA, stimulating TLR3. Aspirate media from cell plates, replace with 90 μL DMEM containing 0.5% FBS in column 2 and 90 μL DMEM containing 0.5% FBS + 50 μg/mg poly I:C in all remaining wells. Compounds diluted to a final working concentration of 30 μM–0.005 μM on cell plates, dosed in triplicate, two columns remain for stimulation with poly I:C, and no stimulation control. Incubate 4.5 h at 37 °C, then add 100 μL of SteadyGlo to each well in the dark. Incubate 15 min. Transfer entire contents of each well, (200 μL), to Corning flat bottomed 96 well white plates. Plates read on Tecan Ultra, data analyzed in Excel.
17. Graczyk, P. P. *J. Med. Chem.* **2007**, *50*, 5773.
18. Bavetsias, V.; Sun, C.; Bouloc, N.; Reynisson, J.; Workman, P.; Linardopoulos, S.; McDonald, E. *Bioorg. Med. Chem. Lett.* **2007**, *17*, 6567.
19. Crystallization, Structure Solution and Refinement: Recombinant protein and crystals were obtained as described (Lawrie, A.M., et al., *Nat. Struct. Biol.* **1997**, *4*, 796–800). Crystals were cross-linked by incubation in mother liquor containing 0.14% glutaraldehyde for 15 min before soaking in 20 mM **4g** overnight in mother liquor containing 20% DMSO. Diffraction data were collected to 2.0 Å resolution in-house on a Rigaku MicroMax007 rotating anode source equipped with a Saturn92 CCD detector. Data were integrated and scaled using d*Trek software (Pflugrath, J. W. *Acta Crystallogr., D* **1999**, *55*, 1718–1725). The structure was determined by molecular replacement using AMoRe (Bailey, S. *Acta Crystallogr., D* **1994**, *50*, 760–763) and refined using Refmac with rebuilding in Coot (Emsley, P., et al. *Acta Crystallogr., D*, **2010**, *66*, 486–501). Waters were added to the structure using Buster (Bricogne G, et al., 2009, BUSTER version 2.8.0. Cambridge United Kingdom: Global Phasing Ltd.) and removed after visual inspection of the electron density. Final refinement statistics converged with $R_{work} = 0.234$ and $R_{free} = 0.303$. The final density surrounding the inhibitor was excellent. The coordinates and structure factors have been deposited in the protein data bank under accession code 3ULI.